Size Attenuated Copper Doped Zirconia Nanoparticles Enhances in Vitro Antimicrobial Properties

Nishakavya S
Chettinad Academy of Research and Education: Chettinad Hospital and Research Institute
Agnishwar Girigoswami
Chettinad Academy of Research and Education: Chettinad Hospital and Research Institute
Deepa R
Chettinad Academy of Research and Education: Chettinad Hospital and Research Institute
Divya A
Chettinad Academy of Research and Education: Chettinad Hospital and Research Institute
Ajith S
Chettinad Academy of Research and Education: Chettinad Hospital and Research Institute
Koyeli Girigoswami (koyelig@gmail.com)
Chettinad Academy of Research and Education: Chettinad Hospital and Research Institute
https://orcid.org/0000-0003-1554-5241

Research Article

Keywords: zirconia, copper doped zirconia, antimicrobial properties, biofilm inhibition, nanoparticles

Posted Date: August 23rd, 2021

DOI: https://doi.org/10.21203/rs.3.rs-807437/v1

Abstract

Biofilm formation hinders the activity of antimicrobial drugs at the site of infections and any agent that can act on both Gram- positive and Gram- bacteria by inhibiting the bacterial growth and rupture the biofilm is needed for the management of infection. In the present study, we have synthesized ZrO_2 NPs and copper doped zirconia nanoparticles (Cu-ZrO_2 NPs) and characterized them using dynamic light scattering, X-ray diffractometry and scanning electron microscopy (SEM). The size of the Cu-ZrO_2 NPs drastically reduced compared to ZrO_2 NPs and the antimicrobial activity was studied against Gram-positive bacteria (*Lactobacillus sp.*) and Gram- negative bacteria (*Pseudomonas aeruginosa*), respectively. The synthesized Cu-ZrO_2 NPs showed superior inhibitory action against *Lactobacillus sp.* compared to ZrO_2 NPs, due to the negatively charged cell wall of *Lactobacillus sp.* which could attract readily the positively charged Cu-ZrO_2 NPs, thereby inhibiting its activity. The biocompatibility was tested using XTT assay in FL cells and the results demonstrated that Cu-ZrO_2 NPs were non- toxic to mammalian cells. Hence, it could be proposed that the synthesized Cu-ZrO_2 NPs possess possible biomedical applications and can be used as antibacterial agents without causing toxicity in mammalian cells.

1. Introduction

The nanoparticles (NPs) engineered from different metal oxides are immensely used in sunscreens, coating with self-cleaning properties, cosmetics, water treatments, paints, polymeric coatings, etc. [1, 2]. The metal oxide NPs have characteristic chemical and physical properties as they have an ultra- small size and a huge density of surfaces and edges, enhancing their surface area. It has been demonstrated by some researchers that metal oxide NPs are also toxic to zebrafishes as well as some organisms [3, 4]. Since the metal oxide NPs exist in a wide range of shape, size, chemical composition and functionalization of surface, they pose a different kind of risks in the organisms. The electronic properties of the material affect the size effect of metal oxides [5]. The semiconducting nature of the metal oxide NPs is due to the bandgap of these NPs which consists of orbitals indicating the electronic structure of a semiconductor. As the NPs size decreases, the number of atoms present on the surface and interface increases and can generate strain or stress resulting in structural perturbation [6].

Zirconium dioxide (ZrO_2) is a refractory and chemically inert metal oxide that exists in several crystalline phases depending on temperature. ZrO_2 has a thermodynamically stable crystalline phase of monoclinic (1170°C), tetragonal (1170–2370°C) and cubic phase (2370–2680°C) under atmospheric pressure [7]. Although the monoclinic phase of ZrO_2 is only thermodynamically stable at room temperature, tetragonal and cubic zirconia can also exist at metastable phases at this temperature. Moreover, because of the low surface energy, the zirconia NPs (ZrO_2 NPs) are preferentially stabilized with the tetragonal structure [8]. The tetragonal phase of ZrO_2 is more valuable for the applications in technology compared to the monoclinic phase, due to its key role in transformation toughening [9]. ZrO_2 exhibits a unique set of properties such as high corrosion resistance, chemical inertness, ionic conductivity, excellent thermal

stability, higher isoelectric point, lack of toxicity, low thermal conductivity, mechanical strength, and good biocompatibility [10–12]. Although the tetragonal structure is very unstable, the most common method of stabilization in the tetragonal phase is the doping of zirconia lattice by bi- or trivalent ions [13]. Zirconia ceramics is becoming an appropriate material for biomedical applications such as hip joint replacement material and dental implants because of white colour and their excellent biocompatibility [14].

ZrO_2 NPs are doped for increasing the stability using metal oxides like Y_2O_3, MgO, CaO, Cr_2O_3, Fe_2O_3, NiO, and CuO yielding cubic and tetragonal phases [15]. Doping with copper to the ZrO_2 NPs can improve its antimicrobial activity which can yield a superior bionanomaterial compared to only ZrO_2 NP. When ZrO_2 NPs are doped with Cu, the process allows stabilizing the tetragonal state, make the surface of the NPs more active to sintering, and reduce the probability of martensitic tetragonal-monoclinic transition during cooling powders from higher temperatures (higher than 1100°C). The durability of ceramic materials can be increased by varying the type or amount of dopants [13]. So far there had been no report on the use of copper doped ZrO_2 NPs (Cu- ZrO_2) to be used as an antimicrobial nanoparticle for its use in biomedicine. Copper NPs are capable to influence the cell membrane by making structural changes, along with bactericidal properties due to the ability of copper to donate and accept electrons continuously.

In the present study, we have synthesized ZrO_2 NPs and Cu-ZrO_2 NPs by sol- gel method and characterized those using different photophysical techniques like dynamic light scattering (DLS), X-ray diffractometry (XRD), and scanning electron microscopy (SEM). The antimicrobial activity and anti-biofilm activity of ZrO_2 NPs and Cu-ZrO_2 NPs were assessed for *P. aeruginosa* and *Lactobacillus sp.*, using turbidity assay and standard crystal violet staining method respectively. The biocompatibility of the synthesized NPs was also assessed by XTT assay using FL cells (HeLa derivative). The purpose of this study was to isolate a superior nanoparticle compared to ZrO_2 NPs with high bacteria- resistant properties.

2. Materials And Methods

2.1 Materials

Zirconium alkoxide, Copper nitrate, Ethanol, nitric acid, DMEM, antibiotics solution (penicillin and streptomycin), Trypsin-EDTA, were procured from Hi media. Fetal bovine serum was purchased from Gibco. FL cells were procured from NCCS, Pune.

2.2. Sol-gel Synthesis of zirconia and copper doped zirconia nanoparticles

The synthesis of ZrO_2 NPs and Cu-ZrO_2 NPs were done according to Asadi et al., (2012) [15], with slight modifications. Zirconium alkoxide (Zr $(OCH_2CH_2CH_3)_4$) was used as a precursor for the synthesis process. To synthesis pure ZrO_2, 4.25 mL zirconium alkoxide was added to 18.75 mL ethanol and then stirred well. Ethanol was used as a media to complete the polymerization uniformly and nitric acid

(HNO_3) was used to adjust the pH (4.0), Further, a mixture of 1.485 mL of distilled water and 6.25 mL ethanol was added slowly to the prior mixture of zirconium alkoxide and ethanol. Then, it was allowed to stir for additional two hours to complete the polymerization and aging process.

To synthesize the Cu-ZrO_2 NPs (5 % doping by copper), 3.705 mL zirconium alkoxide was added to 0.151 g of copper nitrate (Cu $(NO_3)_2.3H_2O$), and further the mixture was stirred in 18.75 mL of ethanol and the pH was adjusted to 4.0 with nitric acid (HNO_3). A mixture of (1.485 mL water and 6.25 mL ethanol) was added slowly to the prior mixture of zirconium alkoxide and ethanol, and then it was allowed to stir for two hours further to complete the polymerization and aging processing. The synthesized ZrO_2 NPs and Cu-ZrO_2 NPs were characterized using UV-visible spectroscopy, DLS, XRD and SEM according to Girigoswami et.al, 2015, 2019 [3, 21].

2.3 Antimicrobial activity assay

The synthesized ZrO_2 NPs and Cu-ZrO_2 NPs were evaluated for inhibition of bacterial growth against both Gram- positive and Gram- negative bacterial strains such as *P aeruginosa* (Gram negative) and *Lactobacillus sp.* (Gram- positive) according to Mftah *et al*., (2015) [22]. UV-visible spectrophotometer (Shimadzu (Japan) UV-1800) was used for this study. The bacterial cultures were maintained on LB agar. These cultures were incubated overnight in 5 mL LB broth at 37°C with shaker speed of 150 rpm until the culture reached an absorbance 1.0 at 600 nm, which corresponds to 10^8 colony forming units per mL.

The antimicrobial activities of the synthesized ZrO_2 NPs and Cu-ZrO_2 NPs were evaluated against the above-mentioned microorganisms, using a turbidity test. For both Gram- positive and Gram-negative bacteria, 4.5 mL of LB broth was taken in test tube and 0.5 ml of the overnight microbial suspension was added in each test tube. Different concentrations (50 µg/mL, 100 µg/mL and 150 µg/mL) of ZrO_2 and Cu-ZrO_2 NPs, only antibiotics (ampicillin for Gram- positive and Streptomycin for Gram- negative) which served as a positive control, were added to the test tubes containing cultures. After incubation of a further 24 h at 37°C, the O.D. at 600 nm was measured. The experiment was performed in triplicate, and the antimicrobial activity was compared between the ZrO_2 NP and Cu- ZrO_2 NP treated bacteria cultures taking the antibiotic- treated O.D. as 100 %.

2.4. Biofilm formation assay

2.4.1 Growing a Biofilm

The wild-type *P. aeruginosa* and *Lactobacillus sp.* culture was grown overnight in an LB medium respectively and used for biofilm formation assay according to O' Toole G.A., 2011 [23]. The overnight culture was diluted to 1:100 into fresh medium for biofilm assays. A standard biofilm assay medium for *P aeruginosa* as well as *Lactobacillus sp.* was used i.e., M63 minimal medium was used which was supplemented with magnesium sulfate casamino acids, and glucose. In 96 well plates, 100 µL diluted bacterial culture was added and was incubated for 72 h at 37 ˚C for the formation of biofilm. We typically used 3 replicate wells for each treatment.

2.4.2. Staining the Biofilm

Post incubation, the cells were discarded by turning the plate upside down and shaking away the liquid, and then submerging the plate in a tray of water. This process was repeated two times to completely remove the unattached cells along with the media components that may get stained, which significantly lowered the background staining. In each well, 125 µL of 0.1 % solution of crystal violet (CV) was added and kept at room temperature for 10–15 min. Further, it was rinsed 3–4 times with water by submerging in a tray of water and blotted vigorously on paper towels stacks to remove the excess cells and dye from the plate. The plate was dried overnight.

2.4.3 Quantifying the Biofilm

The quantification of the biofilm was done by adding 125 µL of 30 % acetic acid in water into each well of the microtiter plate stained the previous day, to solubilize the CV. The microtiter plate was further incubated at room temperature for 10–15 min. 125 µL of the CV which got solubilized was transferred to a new flat-bottomed microtiter dish. Absorbance was measured in a Robonik ELISA plate reader at 550 nm taking 30 % acetic acid as the blank.

2.5 Biocompatibility study using XTT assay

FL cells were maintained in DMEM supplemented with 10 % FBS and 1 % antibiotics at 37°C in a 5 % CO_2 humidified atmosphere as done earlier [21]. 10^4 cells were seeded in 96 well plate and allowed to adhere for 24 h. After 24 h the cells were treated with different concentrations (30 µg/µL, 50 µg/mL, 100 µg/mL, and 150 µg/mL) of ZrO_2 and Cu-ZrO_2 NPs. After 48 h of treatment, the XTT dye was added to the cells under sterile conditions and allowed to incubate at 37°C for 4 h. The metabolically active cells turned the solution orange in color and its O.D. was measured using a Robonik ELISA plate reader at 450 nm. The percentage of viability was calculated as done earlier [21].

3. Results

3.1 Characterization of the synthesized nanoparticles

The synthesized ZrO_2 and Cu- ZrO_2 NPs were characterized photophysically and photochemically for measurement of hydrodynamic diameter and particle stability using zeta sizer, absorbance using UV-visible spectrophotometry, crystal structure using X-ray diffractometry, and surface morphology using scanning electron microscopy. Figure S1 (a) and S1 (b) showed the hydrodynamic diameter of the synthesized NPs with a major scattering peak at 321 nm for ZrO_2 and 240.5 nm for Cu-ZrO_2 respectively. The crystal size of the ZrO_2 and Cu- ZrO_2 were determined using the data obtained by X-ray diffractometry (XRD) according to Meenakshi *et al.*, 2015 [3]. Debye Scherrer equation was used for calculating the crystal size. The crystal size was found to be 84 nm for ZrO_2 NPs (figure S1 (e)) and 108 nm in Cu-ZrO_2 NPs (figure S1 (f)) respectively. The nanoparticle stability can be assessed by using zeta potential values of the NPs when they are suspended in an aqueous solution. We have suspended the

ZrO_2 and Cu-ZrO_2 NPs in water with very high dilutions, ultrasonicated for 20 min two times after a cooling time of 10 min. The particles were taken in plastic cuvettes and inserted with an electrode to measure the zeta potential using Malvern Zeta sizer. The zeta potential of synthesized ZrO_2 and Cu-ZrO_2 NPs was found to be -6.93 mV and + 28.9 mV respectively as shown in figure S1(c and d). The increase in zeta potential values after copper doping shows the high stability of the NPs even after the decrease in their size.

The surface morphology of the synthesized ZrO_2 NPs was visualized using scanning electron microscopy. The NPs are perfectly spherical in shape as seen in Fig. 1 (a). The size of the synthesized zirconia NPs ranged between 175 nm to 200 nm, having an average diameter of nearly 190 nm. The SEM image of copper doped ZrO_2 NPs is shown in Fig. 1 (b). The shape of the NPs is also spherical, and the average diameter is 30 nm. From the SEM images it was clearly indicated that after doping with copper the size of ZrO_2 NPs have reduced nearly 6 times. The absorption spectra of synthesized ZrO_2 is shown in Fig. 1 (c), with a broad absorption range in the UV region. The maximum absorbance was observed at 335 nm, which is attributed to its UV light absorption properties. The Energy-dispersive X-ray spectroscopy (EDS, EDX, EDXS, or XEDS) can be used for the chemical characterization of a sample. To determine whether the synthesis of ZrO_2 NPs was successful without any impurity, the EDX analysis was done. The data so obtained from EDX analysis has spectral peaks that correspond to the different kinds of elements that the sample contains. The ordinate corresponds to the number of counts whereas the abscissa corresponds to the energy of X-rays. Figure 1 (d) shows the EDX analysis of the synthesized ZrO_2 NPs that contains 45.7 wt % Oxygen (O) and 54.3 % Zirconium (Zr). The result shows that the synthesis was done successfully without any impurities.

3.2 Antimicrobial activity

Antimicrobial activity was assessed using turbidity test at different concentrations of ZrO_2 and Cu- ZrO_2 NPs (50µg/ml, 100 µg/ml, 150 µg/ml). The activity was checked against *Lactobacillus sp.* and *P. aeruginosa* (Fig. 2) and the inhibitions were observed in both Gram- negative and Gram- positive bacteria. Compared to ZrO_2 NPs, the Cu- ZrO_2 NPs had higher antimicrobial activity against both *Lactobacillus sp.* and *P. aeruginosa* respectively.

3.3. Biofilm formation assay

The concentration of ZrO_2 and Cu- ZrO_2 NPs for anti-biofilm activity was monitored at 50 µg/ml, 100 µg/ml, and 150 µg/ml (Fig. 3). The biofilm formation was observed in both the bacteria types, *Lactobacillus sp.* and *P. aeruginosa.* The inhibition of biofilm was significantly higher for Cu- ZrO_2 NPs in *Lactobacillus sp.* compared to only ZrO_2 NPs, whereas, the effect on inhibition of biofilm in the case of *P. aeruginosa* was similar for both ZrO_2 and Cu- ZrO_2 NPs at all the doses exploited (no significant difference). The schematic representation of biofilm inhibition is shown in Fig. 4.

3.4 Biocompatibility assay

The exposure of FL cells to the different concentrations of ZrO_2 and Cu- ZrO_2 NPs (30 µg/ml, 50 µg/ml, 100 µg/ml and 150 µg/ml) is shown in Fig. 5. The data shows that the ZrO_2 NPs were toxic to the cells at a low dose but as the dose increased the toxicity was reduced. On the other hand, Cu- ZrO_2 NPs were not toxic to the FL cells at the different doses used. The decrease in toxicity of the ZrO_2 NPs at a high dose may be attributed to the aggregation of the NPs, which did not enter the cells to exert their toxicity. Thus, it was safe to use Cu- ZrO_2 NPs for their insignificant toxicity.

4. Discussion

We have successfully synthesized ZrO_2 NPs and characterized them using different photophysical tools. To incorporate antimicrobial activity to the synthesized ZrO_2 NPs along with its other properties like increased microhardness, its strong interaction with active phase, high thermal stability, chemical inertness, etc., we have doped the ZrO_2 NPs with a small amount of Cu (5 %) and wanted to study their antimicrobial activity and biocompatibility. The synthesis of ZrO_2 NPs and Cu-ZrO_2 NPs was done using the sol- gel method and was characterized using UV-visible spectroscopy, FTIR, DLS, zeta potential, SEM imaging, and EDX analysis. The XRD data showed the crystal size of ZrO_2 NPs was 84 nm and for Cu-ZrO_2 NPs 108 nm. The noise obtained in the XRD pattern shows the partial amorphous nature of the ZrO_2-NPs and Cu- ZrO_2 NPs (figure S1 (e) and (f)). This may be attributed to the low calcination temperature that we have used (200°C) during synthesis. The typical peaks obtained for ZrO_2 NPs at 2θ value of 30 ° and 51 ° corroborates with the JCPDS pattern of ZrO_2 (cubic ZrO_2-27-0997 and tetragonal ZrO_2-80-0965). The two pictures showed that after doping with Cu to the ZrO_2 NPs, the crystal size has increased compared to ZrO_2. Dopants affect grain growth, and it is due to the strain in the lattice of compounds the size increases. In some studies, it has been found that the size of the crystallites of alkali-treated zirconia which was calculated from data obtained by XRD was around the range of 15–33 nm [8]. A similar XRD pattern was found in previous studies also which showed a combination of both tetragonal and monoclinic structures, similar to our finding [25]. The absorbance spectrum of ZrO_2 NPs showed a wide peak in the UV region with a λ_{max} of 335 nm (Fig. 1 (c)). Previous studies have also shown that the absorption spectrum of microwave synthesized ZrO_2 NPs have a wide absorption peak in the UV region [26]. Thus, the characteristic peak of ZrO_2 NPs was obtained supporting its synthesis. The hydrodynamic diameter of both ZrO_2 NPs and Cu-ZrO_2 NPs was monitored to assess their size. The hydrodynamic diameter of ZrO_2 NPs and Cu-ZrO_2 NPs was 321 nm and 240 nm respectively as obtained by DLS studies (figure S1(a) and (b)). The findings of DLS studies showed that the size of NPs reduced after doping with Cu. The incorporation of Cu may strain the lattice of the ZrO_2 NPs and reduce the size having a higher affinity for oxygen.

To further exploit the stability of the NPs the zeta potential of synthesized ZrO_2 NPs and Cu-ZrO_2 NPs was observed. Zeta potential is taken as a measure to evaluate the stability of NPs [3]. The zeta potential

of ZrO_2 NPs and Cu-ZrO_2 NPs was − 6.9 mV and + 28.9 mV respectively (figure S1(c) and (d)). The results showed that even though the size of the NPs has reduced but it has increased the stability. This shows that Cu-ZrO_2 can be a superior nanoparticle compared to only ZrO_2, based on its small size and high stability. The surface morphology of ZrO_2 NPs and Cu-ZrO_2 NPs and the chemical composition of ZrO_2 NPs were monitored using SEM analysis (Fig. 1 (a) and (b) and EDX analysis (Fig. 1 (d)) respectively. The shape of both ZrO_2 NPs and Cu-ZrO_2 NPs was spherical, but the diameter was nearly 178 nm for ZrO_2 NPs and 30 nm for Cu-ZrO_2 NPs. The SEM results corroborated with our findings of DLS studies where we found that the hydrodynamic diameter of Cu-ZrO_2 NPs was reduced compared to only ZrO_2 NPs. The chemical composition of ZrO_2 NPs was analysed using EDX. The data showed that the peaks obtained by the EDX correspond to Zr and O. Thus, there was minimum impurity present in the synthesized ZrO_2 NPs and our synthesis was successful.

In our study, antimicrobial activity using turbidity test of ZrO_2 NPs and Cu- ZrO_2 NPs showed the inhibitory action for both Gram- positive (*Lactobacillus sp.*) and Gram- negative bacteria (*P aeruginosa*) (Fig. 2). The physicochemical characteristics of surfaces of specific materials are reported to influence the process of bacterial adhesion significantly [27]. Our results with Cu- ZrO_2 NPs also showed significant antimicrobial activity against *P aeruginosa* and *Lactobacillus sp.* and we can propose that this nanoparticle can be used as an effective biomaterial with antimicrobial property. Zn and Cu have been reported to have a potential anti-biofilm capability and this property was useful to prevent biofilm formation synergistically against *S mutans* and *Streptococcus sanguinis* [30]. Our results for the assessment of anti- biofilm formation showed that ZrO_2 NPs and Cu- ZrO_2 NPs showed inhibition of biofilm formation against both bacteria *Lactobacillus sp.* and *P aeruginosa* respectively (Fig. 3). The inhibition was significantly higher for Cu- ZrO_2 NPs against Lactobacillus. *sp.* than only ZrO_2 NPs and is schematically illustrated in Fig. 4. Moreover, the biocompatibility of these synthesized NPs was needed to be assessed because any agent which will come in contact with biological fluids needs to be biocompatible. The *in vitro* cell culture study showed that Cu-ZrO_2 NPs did not show any significant toxicity against FL cells when treated with low as well as high doses (Fig. 5). Although, the ZrO_2 NPs were found to be toxic at low doses (50 µg/mL), but non- toxic at high doses. The toxicity at a low dose may be attributed to its ultrasmall size which could enter the cells and exhibit its toxicity. At high doses there are possibilities of aggregation of the ZrO_2 NPs, and they may not enter the cells to elicit the toxic response. Thus, from our results, it can be concluded that doping of ZrO_2 NPs with Cu yielded a superior ZrO_2 NPs, which has unique properties of killing both Gram-positive as well as Gram-negative bacterial cells and could also inhibit the biofilm formation against *Lactobacillus sp.* Further studies are required to be done with other strains of bacteria and explore their efficacy in killing these bacteria, inhibiting biofilm formation.

5. Conclusion

We have shown that ZrO_2 NPs and Cu- ZrO_2 NPs were synthesized by the sol- gel method and characterized with various analytical techniques. The XRD study of pure ZrO_2 NPs and Cu- ZrO_2 NPs shows that both the synthesized particles are amorphous in nature, although the crystal size increase due to copper doping ensures that the doping is done successfully. The stability also increased after doping as revealed by the increase in zeta potential. Antimicrobial studies revealed that ZrO_2 NPs and Cu-ZrO_2 NPs both inhibited microbial growths as tested against the Gram- positive and Gram- negative bacteria, Cu-ZrO_2 being more effective at the doses used. The biofilm formation was also found to be inhibited by both the NPs without showing any significant difference in inhibition. The study showed that Cu doping in ZrO_2 NPs could enhance the protection against bacteria and thereby can be proposed as a superior antibacterial agent compared to only ZrO_2 NPs. The toxicity study of ZrO_2 NPs and Cu-ZrO_2 NPs in FL cells showed that Cu-ZrO_2 NPs were much more biocompatible to mammalian cells and can be safely used as a component for biomedical implants inside our body.

Declarations

Acknowledgement

The authors are grateful to Chettinad Academy of Research and Education for providing the infrastructural support. The authors acknowledge funding from Council of Scientific and Industrial Research (CSIR), INDIA, Scheme No. 01(2868)/17/EMR-II.

Conflicts of Interest

The authors declare no conflict of interest.

Funding: The study was funded by Council of Scientific and Industrial Research (CSIR), INDIA, Scheme No. 01(2868)/17/EMR-II.

Conflicts of interest/Competing interests:

- The authors have no relevant financial or non-financial interests to disclose.
- The authors have no conflicts of interest to declare that are relevant to the content of this article.
- All authors certify that they have no affiliations with or involvement in any organization or entity with any financial interest or non-financial interest in the subject matter or materials discussed in this manuscript.
- The authors have no financial or proprietary interests in any material discussed in this article.

Availability of data and material: All the authors declare that all data and materials support their published claims and comply with field standards.

Informed consent statement: Not applicable

Ethical consent:

- The manuscript is not be submitted to more than one journal for simultaneous consideration.
- The submitted work is original and should not have been published elsewhere in any form or language (partially or in full).
- A single study is not split up into several parts to increase the quantity of submissions and submitted to various journals or to one journal over time (i.e. 'salami-slicing/publishing').
- Results are presented clearly, honestly, and without fabrication, falsification or inappropriate data manipulation (including image based manipulation). Authors have adhered to discipline-specific rules for acquiring, selecting and processing data.
- No data, text, or theories by others are presented as if they were the author's own ('plagiarism'). Proper acknowledgements to other works have been given.

Authors' contributions: Nishakavya S, Divya A, Deepa R, Ajith S have executed the experiments. Agnishwar Girigoswami and Koyeli Girigoswami have given the concept, and prepared the final manuscript.

Code availability-Not Applicable

Consent to participate-Yes

Consent for publication-Yes

References

1. Puzyn, T., Rasulev, B., Gajewicz, A., Hu, X., Dasari, T. P., Michalkova, A., Hwang, H. M., Toropov, A., Leszczynska, D. and Leszczynski, J.: Using nano-QSAR to predict the cytotoxicity of metal oxide nanoparticles, Nat. Nanotechnol., **6**, 175-178 (2011).

2. Sung, L-P., Scierka, S., Baghai-Anaraki, M. and Ho, D. L.: Characterization of metal-oxide nanoparticles: synthesis and dispersion in polymeric coatings, 2003 Mat. Res. Soc. Symp. Proc., **7401**, 15.4.1-15.4.6 (2003).

3. Girigoswami, K., Viswanathan, M., Murugesan, R. and Girigoswami, A.: Studies on polymer-coated zinc oxide nanoparticles: UV-blocking efficacy and in vivo toxicity, Mater. Sci. Eng. C, **56**, 501-510 (2015).

4. Dreher, K. L.: Health and environmental impact of nanotechnology: toxicological assessment of manufactured nanoparticles, Toxicol. Sci., **77**, 3-5 (2004).

5. Aricò, A., Bruce, P., Scrosati, B., Tarascon, J-M., van Schalkwijk, W.: Nanostructured materials for advanced energy conversion and storage devices, Nature Mater., **4**, 366-377 (2005).

6. Song, Z., Cai, T., Chang, Z., Liu, G., Rodriguez, J. A. and Hrbek, J.: Molecular level study of the formation and the spread of MoO3 on Au(111) by scanning tunneling microscopy and X-ray photoelectron spectroscopy, J. Am. Chem. Soc., **125**, 8059-8066 (2003).

7. Lim, H., Ahmad, A. and Hamzah, H.: Synthesis of zirconium oxide nanoparticle by sol-gel technique, AIP Conference Proceedings, **1571**, 812 (2013). https://doi.org/10.1063/1.4858755

8. Behbahani, A., Rowshanzamir, S. and Esmaeilifar, A.: Hydrothermal synthesis of zirconia nanoparticles from commercial zirconia, Procedia Engineering, **42**, 908-917 (2012)

9. Geuzens, E., Vanhoyland, G., D'Haen, J., Van Bael, M. K., Van den Rul, H., Mullens, J. and Van Poucke, L. C.: Synthesis of tetragonal zirconia nanoparticles via an aqueous solution-gel method, Key Engineering Materials, **264–268**, 343-346 (2004).

10. Maridurai, T., Balaji, D. and Sagadevan, S.: Synthesis and characterization of yttrium stabilized zirconia nanoparticles, Materials Res., **19**, 812-816 (2016).

11. Thakare, V., Joshi, P., Godse, R., Bhatkar, V., Wadegaokar, P. and Omanwar, S. K.: Evaluation of biological activities of nanocrystalline tetragonal zirconia synthesized via sol-gel method, Int. J. Pharmacy Pharmaceut. Sci., **8**, 125-131 (2016).

12. Gupta, P. K., Pachauri, N., Khan, Z. H. and Solanki, P. R.: One pot synthesized zirconia nanoparticles embedded in amino functionalized amorphous carbon for electrochemical immunosensor, J. Electroanal. Chem., **807**, 59- 69(2017).

13. Lakusta, M., Danilenko, I., Konstantinova, T. and Volkova, G.: Influence of obtaining conditions on kinetics of the initial sintering stage of zirconia nanopowders, Nanoscale Res. Lett., **11**, 238 (2016). doi: 10.1186/s11671-016-1452-3.

14. Chen, Y.W., Moussi, J., Drury, J.L. and Wataha, J.C.: Zirconia in biomedical applications, Expert Rev. Med. Devices, **13(10)**, 945-963 (2016).

15. Asadi, S., Abdizadeh, H. and Vahidshad, Y.: Effect of crystalline size on the structure of copper doped zirconia nanopaticles synthesized via sol-gel, J. Nanostructures, **2(2)**, 205-212 (2012).

16. Girigoswami, A., Ramalakshmi, M., Akhtar, N., Metkar., S. K. and Girigoswami, K.: ZnO Nanoflower petals mediated amyloid degradation - an in vitro electrokinetic potential approach, Mater. Sci. Eng. C, **101**, 169-178 (2019).

17. Mftah, A., Alhassan, F. H., Al-Qubaisi, M. S., El Zowalaty, M. E., Webster, T. J., Sh-Eldin, M., Rasedee, A., Taufiq-Yap, Y. H. and Rashid, S. S.: Physicochemical properties, cytotoxicity, and antimicrobial activity of sulphated zirconia nanoparticles, Int. J. Nanomedicine., **10**, 765- 774 (2015).

18. O'Toole, G. A.: Microtiter dish biofilm formation assay, J. Vis. Exp., **47**, 2437 (2011).

19. Chikere, C. O., Faisal, N. H,, Kong-Thoo-Lin, P. and Fernandez, C.: Interaction between amorphous zirconia nanoparticles and graphite: electrochemical applications for gallic acid sensing using carbon paste electrodes in wine, Nanomaterials (Basel) **10**, 537 (2020).

20. Singh, A. K. and Nakate, U. T.: Microwave synthesis, characterization, and photoluminescence properties of nanocrystalline zirconia, Scientific World J., **2014**, 349457 (2014).

21. Cabal, B., Cafini, F., Esteban-Tejeda, L., Alou, L., Bartolomé, J. F., Sevillano, D., López-Piriz, R., Torrecillas, R. and Moya, J. S.: Inhibitory effect on in vitro Streptococcus oralis biofilm of a soda-lime glass containing silver nanoparticles coating on titanium alloy, PLoS One, **7**, e42393 (2012).

22. Afra, S. M. and Modaresi, F.: The use of synergistically antiplaque nanoparticles in treating dental caries, J. Dent. Oral Disord. Ther., **6,** 00214 (2017).

Figures

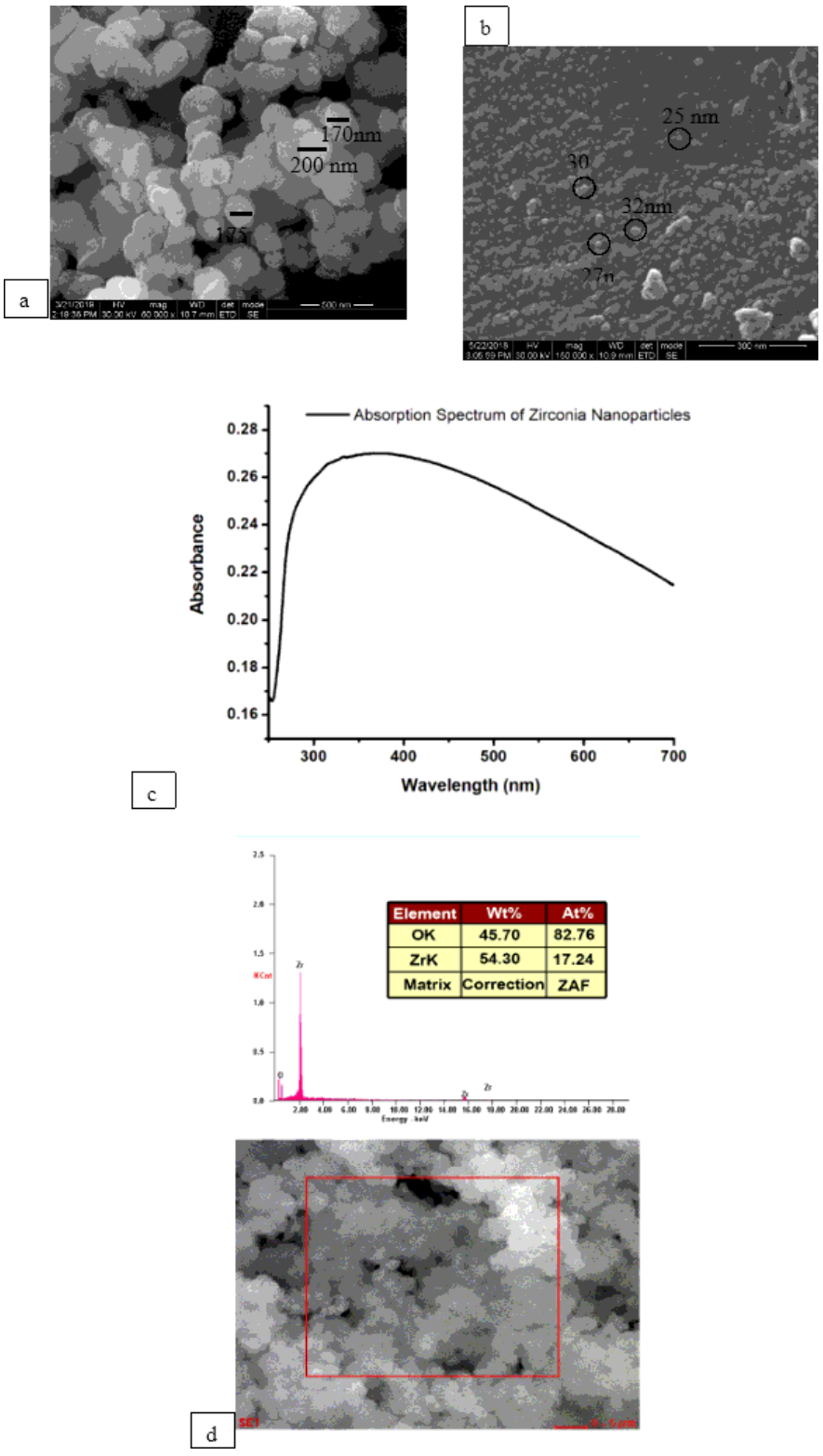

Figure 1

The SEM image of (a) ZrO2 nanoparticles, (b) Cu- ZrO2 nanoparticles. The absorption spectra (c) and EDAX (d) of ZrO2 nanoparticles

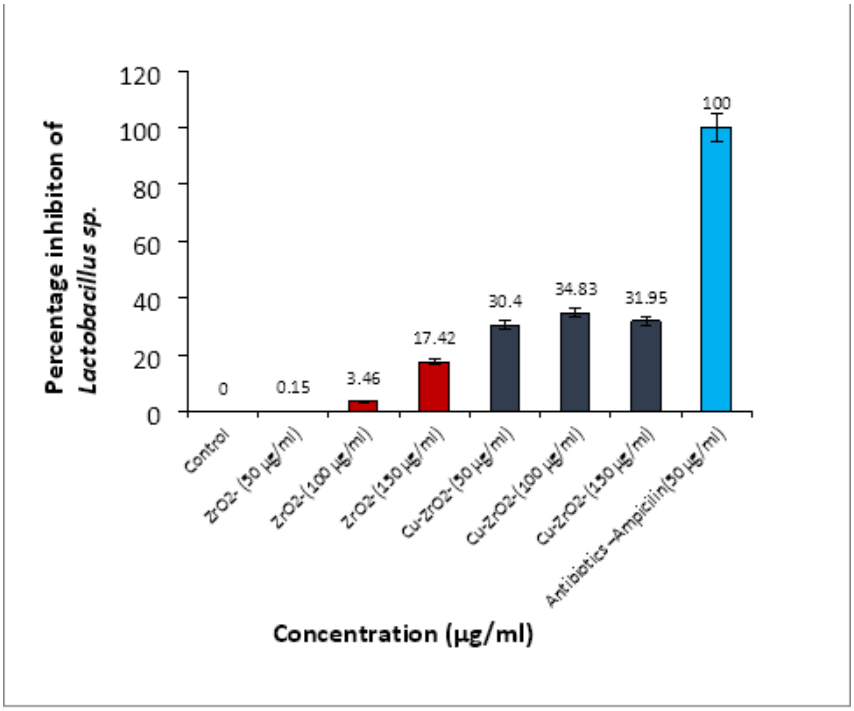

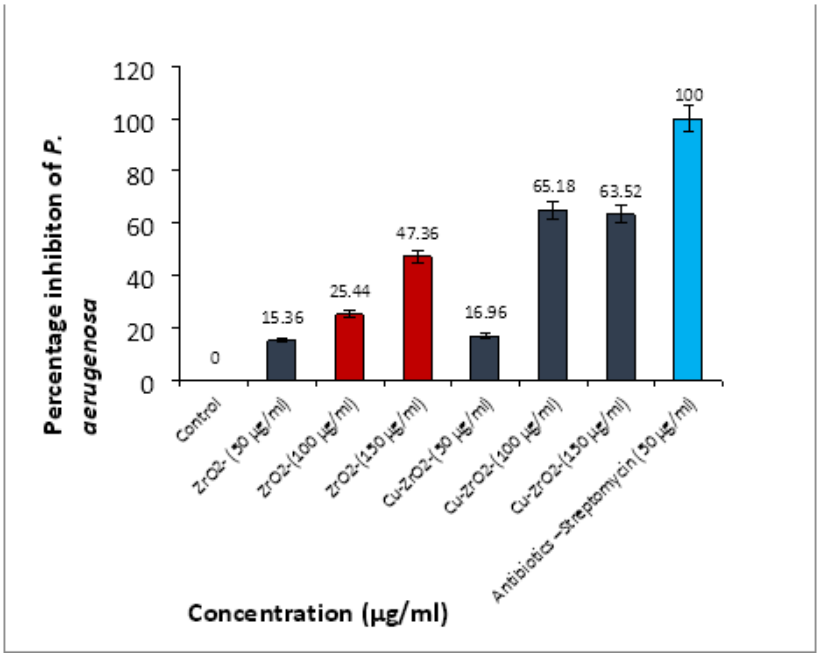

Figure 2

Antimicrobial activity of ZrO2 and Cu-ZrO2 nanoparticles at different doses (50, 100 and 150 µg/mL) against Lactobacillus sp. and P. aeruginosa

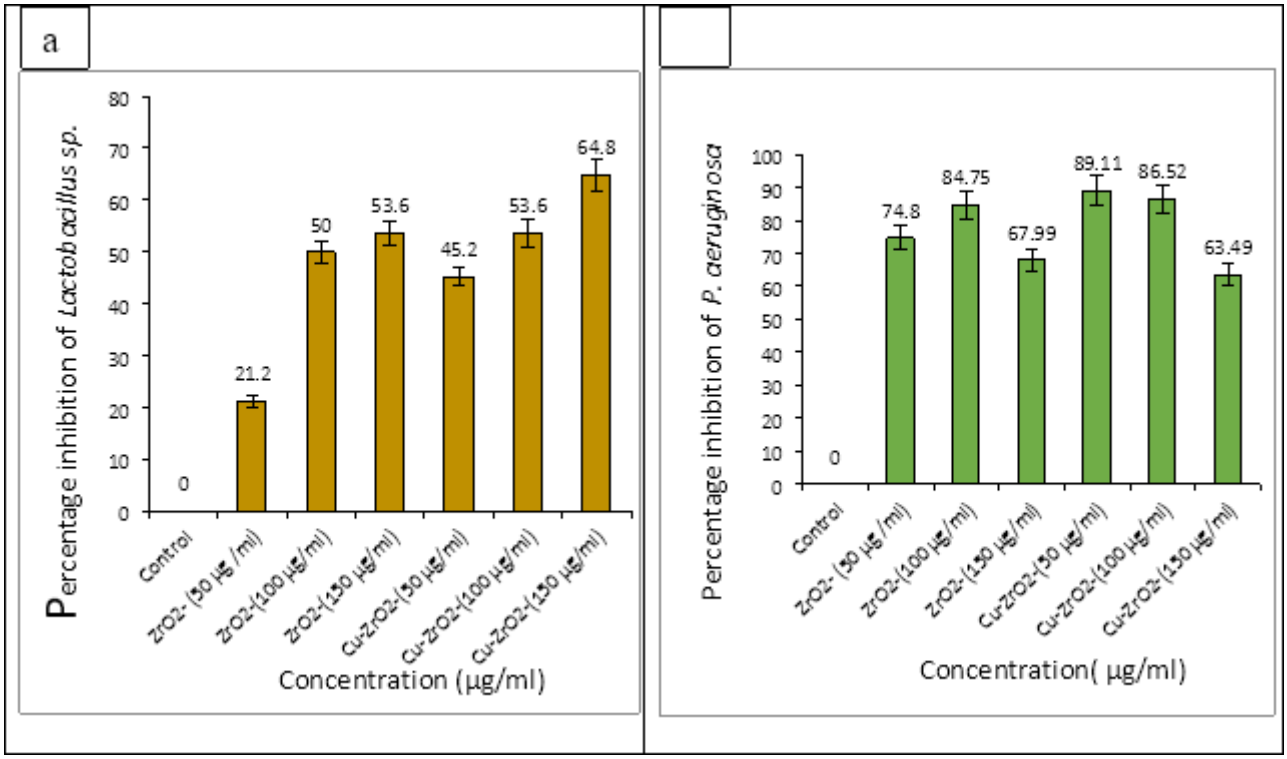

Figure 3

The percentage inhibition of bioflim formation by (a) ZrO2 and (b) Cu- ZrO2 nanoparticles at different concentrations (50, 100 and 150 µg/mL) for Lactobacillus sp. and P. aerugenosa

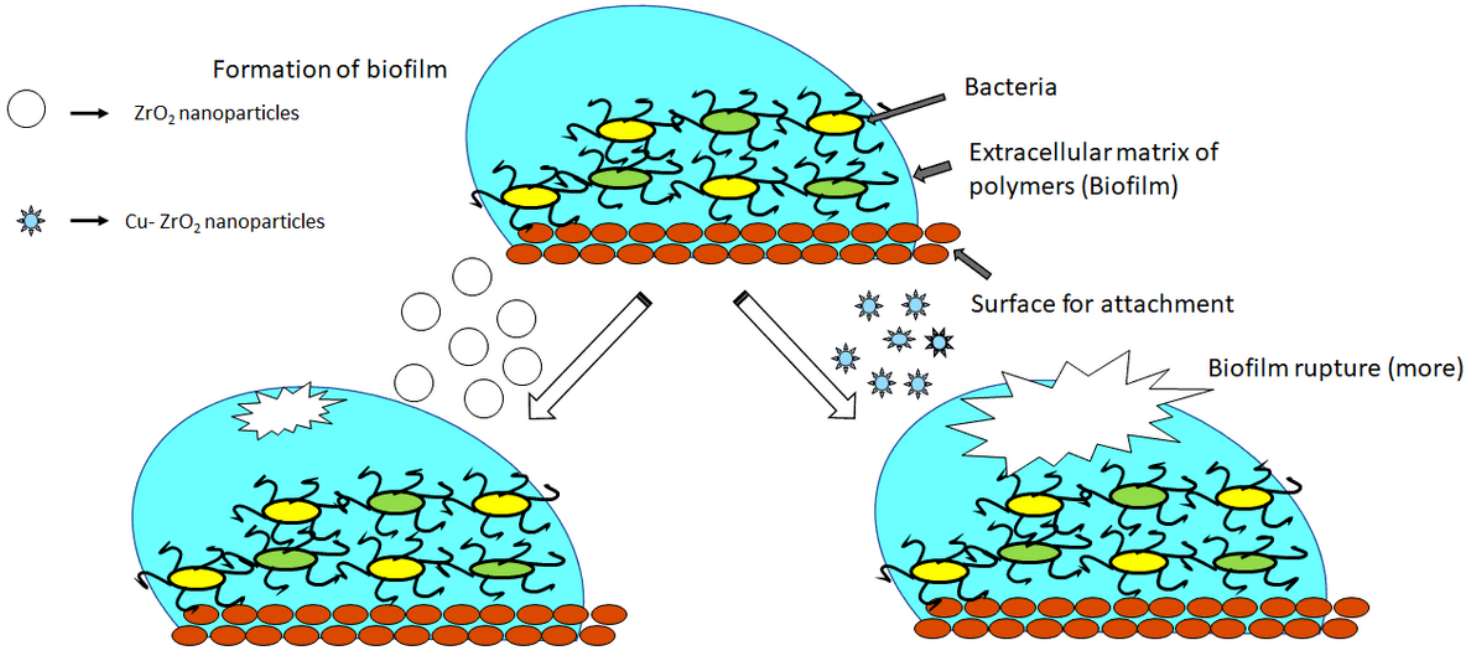

Figure 4

Scheme showing the destruction of bacterial biofilm by ZrO2 nanoparticles and Cu-ZrO2 nanoparticles

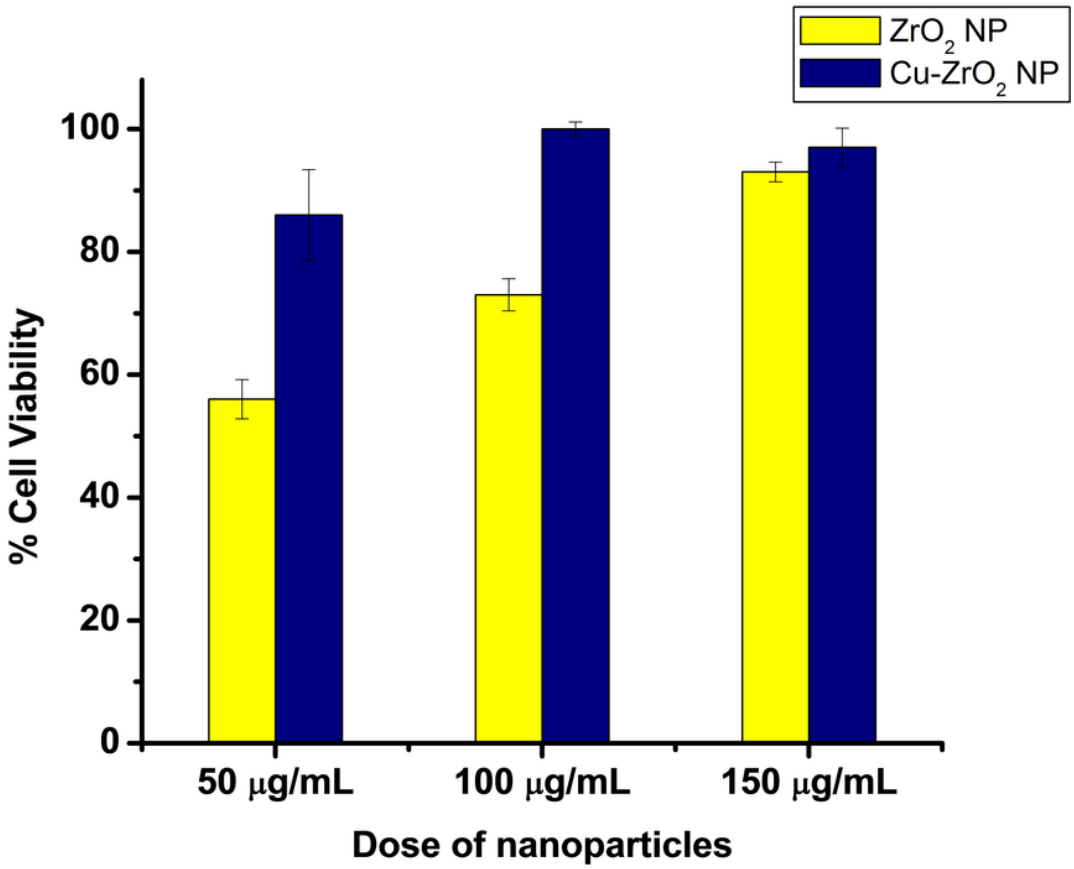

Figure 5

The cell viability assessed using XTT assay for FL cells after treatment with ZrO2 and Cu- ZrO2 nanoparticles at different doses.

Supplementary Files

This is a list of supplementary files associated with this preprint. Click to download.

- SuppleS1.docx